Economic Evaluation of Three-Phase Imbalance Mitigation Considering Optimal ESS Sizing in Distribution Systems

Donghyun Yoon, Dongwon Lee, Jaesung Jung*
Dept of Electronical and computer Engineering
Ajou University
Suwon, South Korea
ydh812@ajou.ac.kr, memo7978@ajou.ac.kr, jjung@ajou.ac.kr

***Abstract*—Power distribution systems are inherently limited in maintaining three-phase balance. Moreover, the imbalance has intensified with the rapid integration of new load devices and distributed power sources. Therefore, this study proposes an ESS operation algorithm to mitigate three-phase current imbalance. In addition, an optimal ESS sizing method is introduced that incorporates the economic impact of imbalance mitigation. To minimize the imbalance, a mathematical objective function is formulated to determine the required compensation energy of the ESS. The optimal ESS set-point is calculated based on complex power control constraints. To verify the balancing performance, the proposed algorithm is simulated using actual load and generation data from the IEEE 34-bus test system. To determine the optimal sizing, the economic feasibility is evaluated by considering both imbalance-mitigation savings and ESS wear-out costs. Through a comparative analysis of imbalance and economic indicators, the economic effectiveness of ESS-based three-phase imbalance mitigation is verified.**

***Index Terms*-- Three-phase current-balancing operation; Energy storage system; Optimal ESS sizing; Optimal power calculation; Economic analysis.**

I. INTRODUCTION

Recently, power generation has shifted from fossil fuels to inverter-based resources, such as photovoltaics (PVs), while emerging loads like electric vehicles are rapidly changing consumption patterns [1]. Consequently, these changes have gradually worsened the imbalance in distribution systems, which are inherently limited in maintaining three-phase balance. An increase in the degree of three-phase imbalance leads to higher power losses and harmonic distortion [2]. Furthermore, many system components, such as substation transformers, are designed under the assumption of three-phase balance; thus, the imbalance directly reduces their lifetime and efficiency [3].

To mitigate the imbalance effectively, both the supply and absorption of active and reactive power through bidirectional control are required in distribution systems [4]. To address this need, energy storage systems (ESSs) with a fast response and bidirectional P/Q control offer an effective solution. The ESS can mitigate the increasing imbalance in distribution systems; however, this application has not been extensively studied. Most existing ESS applications have focused solely on mitigating imbalance at the local level in combination with individual resources such as PVs [5]-[6]. Moreover, detailed calculations of ESS operations required for imbalance mitigation have not been provided. Therefore, further development is needed to employ ESSs for phase-balancing operations in distribution systems.

Despite these advantages, ESSs have historically shown limited cost-effectiveness due to high installation and maintenance expenses. However, the cost of ESSs has significantly decreased in recent years, and this downward trend is expected to continue [7]. Moreover, phase redistribution for imbalance correction incurs labor and customer-interruption costs, while the imbalance itself accelerates transformer degradation, leading to additional maintenance and outage costs [3], [8]-[9]. When the reduction in power loss through imbalance mitigation is also considered, the use of ESSs for three-phase imbalance mitigation can be regarded as economically feasible.

Therefore, this study proposes an ESS-based operation algorithm for three-phase current imbalance mitigation and systematically evaluates its optimal sizing and economic feasibility. In this study, the ESS operation is formulated to focus on imbalance from an operational perspective, without simultaneously addressing multiple operational objectives. The optimal ESS sizing is subsequently determined by incorporating the economic impact of imbalance mitigation. The optimal compensation energy of the ESS is derived through a nonlinear optimization model formulated using symmetrical component currents as the objective function. To verify the proposed algorithm, case studies are conducted using actual

979-8-3315-8138-1

load and generation profiles from the IEEE 34-bus test system in the scheduling operation. The economic feasibility of ESS operation is then evaluated based on the optimal capacity obtained from the economic analysis of imbalance mitigation. The main contributions of this study are summarized as follows: (1) Development of a nonlinear optimization model for three-phase imbalance mitigation, formulated using symmetrical component currents and numerically solved to derive the optimal ESS set-points. (2) Determination of the optimal ESS capacity by incorporating the economic impact of three-phase imbalance, accounting for both imbalance-mitigation savings and battery degradation costs.

II. Objective Function Design For Three Phase Balancing

A. Network model for ESS operation

This study aims to install an ESS at any location where the system imbalance is significant; thus, its operational effect will be greater. For this purpose, a simple network model is used to simplify the complex and large distribution system, as shown in Fig. 1.

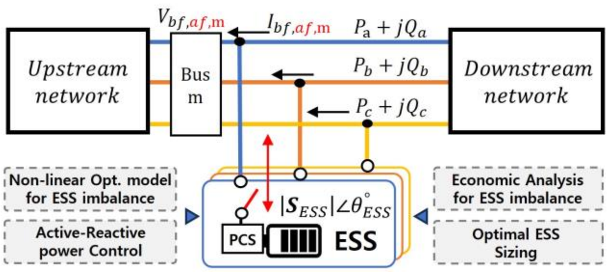

Figure 1. Network model for ESS operation.

We assume that the system can measure the current difference between each phase and that the ESS consumes or supplies its energy to balance the phase current at bus m. Before the operation of the ESS, the power flow ($\boldsymbol{S}_{bf}$) can be represented as follows:

$$\boldsymbol{S}_{bf} = P + jQ = \boldsymbol{V}_{bf}\boldsymbol{I}_{bf}^{*}, \tag{1}$$

where $\boldsymbol{V}_{bf}$ is the voltage to the ground and $\boldsymbol{I}_{bf}$ is the line current and P_{bf}, Q_{bf} denotes the active and reactive power flow at bus m. Although the current flows toward the downstream network, for simple derivation, the opposite direction is used. After the operation of the ESS, the power flow ($\boldsymbol{S}_{af}$) is changed to:

$$\boldsymbol{S}_{af} = \boldsymbol{S}_{bf} + \boldsymbol{S}_{ESS} = P + P_{ESS} + j(Q + Q_{ESS}) \tag{2}$$

where $\boldsymbol{V}_{af}$ is the updated voltage to the ground and $\boldsymbol{I}_{af}$ is the updated line current after the operation of the ESS at bus m. After ESS operation, the marginal change in the power flow ($\boldsymbol{S}$) is ignored. To determine the optimal compensation energy by the ESS, the equation is rearranged in terms of the current ($\boldsymbol{I}_{af}$) and then represented by the ESS power flow (P_{ESS}, Q_{ESS}) by denoting the voltage coefficients at bus m as V_r, V_i:

$$\boldsymbol{I}_{af} = \left(\frac{\boldsymbol{S}_{af}}{\boldsymbol{V}_{af}}\right)^{*} = \left(\frac{P + P_{ESS} + j(Q + Q_{ESS})}{V_{af,r} + jV_{af,i}}\right)^{*} \tag{3}$$

$$\boldsymbol{I}_{af} = \boldsymbol{I}_{bf} + V_r P_{ESS} + V_i Q_{ESS} + j(V_i P_{ESS} - V_r Q_{ESS}) \tag{4}$$

where, $\boldsymbol{V}_{af} = V_{af,r} + jV_{af,i}$, $V_r = \frac{V_{af,r}}{(V_{af,r}^2 + V_{af,i}^2)}$, $V_i = \frac{V_{af,i}}{(V_{af,r}^2 + V_{af,i}^2)}$.

Therefore, the updated current ($\boldsymbol{I}_{af}$) after ESS operation can be represented by the control variables (P_{ESS}, Q_{ESS}) and the measurements values ($\boldsymbol{I}_{bf}$, V_r, V_i).

B. Objective function with symmetrical component

Some studies on three-phase imbalance rely only on limited factors such as voltage and current magnitudes without considering phase angles, which limits their ability to accurately evaluate a balanced three-phase condition. Therefore, this paper employs the symmetrical component method to formulate the objective function by jointly accounting for both magnitude and phase angle information of the three phases. The $\boldsymbol{I}_{af}$ can be converted into symmetrical components as follows:

$$\begin{bmatrix} \boldsymbol{I}_{af}^{(0)} \\ \boldsymbol{I}_{af}^{(+)} \\ \boldsymbol{I}_{af}^{(-)} \end{bmatrix} = \frac{1}{3}\begin{bmatrix} 1 & 1 & 1 \\ 1 & \boldsymbol{a} & \boldsymbol{a}^2 \\ 1 & \boldsymbol{a}^2 & \boldsymbol{a} \end{bmatrix}\begin{bmatrix} \boldsymbol{I}_{af,a} \\ \boldsymbol{I}_{bf,b} \\ \boldsymbol{I}_{bf,c} \end{bmatrix} \tag{5}$$

where $\boldsymbol{I}_{af}^{(0)}, \boldsymbol{I}_{af}^{(+)}$, and $\boldsymbol{I}_{af}^{(-)}$ represent the zero-, positive-, and negative-sequence current, respectively, and $\boldsymbol{a}$=1.0∠120°. Here, the selected phase-line current ($\boldsymbol{I}_{af,a}$) is derived based on phase A, as (5). The phase currents of the unselected phases ($\boldsymbol{I}_{bf,b}, \boldsymbol{I}_{bf,c}$) are obtained from the previous iterations and measured values. If the selected operating phase changes in the next iteration, the phase current values in (5) are also updated accordingly. By substituting (4) into (5), the following symmetrical component current is calculated:

$$\boldsymbol{I}_{af}^{(0)} = \frac{1}{3}\left\{3\boldsymbol{I}_{bf}^{(0)} + V_r P_{ESS} + V_i Q_{ESS} + j(V_i P_{ESS} - V_r Q_{ESS})\right\} \tag{6}$$

$$\boldsymbol{I}_{af}^{(-)} = \frac{1}{3}\left\{3\boldsymbol{I}_{bf}^{(-)} + V_r P_{ESS} + V_i Q_{ESS} + j(V_i P_{ESS} - V_r Q_{ESS})\right\} \tag{7}$$

$$\boldsymbol{I}_{af}^{(+)} = \frac{1}{3}\left\{3\boldsymbol{I}_{bf}^{(+)} + V_r P_{ESS} + V_i Q_{ESS} + j(V_i P_{ESS} - V_r Q_{ESS})\right\} \tag{8}$$

where, $\boldsymbol{I}_{bf}^{(0)} = \frac{1}{3}(\boldsymbol{I}_{bf,a} + \boldsymbol{I}_{bf,b} + \boldsymbol{I}_{bf,c})$,
$\boldsymbol{I}_{bf}^{(-)} = \frac{1}{3}(\boldsymbol{I}_{bf,a} + \boldsymbol{a}^2\boldsymbol{I}_{bf,b} + \boldsymbol{a}\boldsymbol{I}_{bf,c})$,
$\boldsymbol{I}_{bf}^{(+)} = \frac{1}{3}(\boldsymbol{I}_{bf,a} + \boldsymbol{a}\boldsymbol{I}_{bf,b} + \boldsymbol{a}^2\boldsymbol{I}_{bf,c})$.

The system is assumed to be balanced if two conditions are satisfied: the magnitude of each phase current is identical, and the difference in the phase angle between each phase current is 120°. Therefore, the objective function is determined to minimize the magnitudes of both the zero- and negative-sequence components of the phase-line current as follows:

$$Objective\ function = \min\left\{\left|\boldsymbol{I}_{af}^{(0)}\right|^2 + \left|\boldsymbol{I}_{af}^{(-)}\right|^2\right\}. \tag{9}$$

By substituting (6) and (7) into (9), the objective function can be calculated as follows:

$$\begin{aligned} &Objective\ function = f(P_{ESS}, Q_{ESS}) \\ &= \min\{\alpha P_{ESS}^2 + \alpha Q_{ESS}^2 + \beta_p P_{ESS} + \beta_q Q_{ESS} + \gamma\} \end{aligned} \tag{10}$$

where, $\boldsymbol{I}_{bf}^{(0)} = I_{bf,re}^{(0)} + jI_{bf,im}^{(0)}$, $\boldsymbol{I}_{bf}^{(-)} = I_{bf,re}^{(-)} + jI_{bf,im}^{(-)}$,
$\alpha = \frac{2}{9}(V_r^2 + V_i^2)$,
$\beta_p = \frac{2}{3}\left\{V_r(I_{bf,re}^{(-)} + I_{bf,re}^{(0)}) + V_i(I_{bf,im}^{(-)} + I_{bf,im}^{(0)})\right\}$,
$\beta_q = \frac{2}{3}\left\{V_i(I_{bf,re}^{(-)} + I_{bf,re}^{(0)}) - V_r(I_{bf,im}^{(-)} + I_{bf,im}^{(0)})\right\}$,
$\gamma = \left\{{I_{bf,re}^{(-)}}^2 + {I_{bf,im}^{(-)}}^2 + {I_{bf,re}^{(0)}}^2 + {I_{bf,im}^{(0)}}^2\right\}$.

The objective function is now represented by a quadratic equation that includes the active and reactive power flows of

979-8-3315-8138-1

ESS (P_{ESS}, Q_{ESS}). Here, the objective-function coefficients (α, β_p, β_q, γ) and its terms are coefficient parameters that are updated from the results of the power-flow analysis. By partially differentiating (10) with respect to P and Q, the solutions can be obtained and expressed as shown in (11).

$$P_{opt} = -\frac{\beta_p}{2\alpha}, \; Q_{opt} = -\frac{\beta_q}{2\alpha} \tag{11}$$

The ESS can control the complex power of the ESS ($\boldsymbol{S}_{ESS}$) through the reactive power control of the smart inverter in the power-conversion system (PCS). To determine the optimal ESS set points, the $\boldsymbol{S}_{ESS}$ can be calculated as follows:

$$\boldsymbol{S}_{ESS} = P_{opt} + jQ_{opt} = |\boldsymbol{S}_{ESS}|\angle\theta_{ESS}^{\circ} \tag{12}$$

The maximum power of the ESS ($|\boldsymbol{S}_{limit}|$) is determined by the PCS rating, SOC, and voltage–current limits. If the SOC of the ESS is sufficient to charge or discharge the calculated complex power, the maximum rating of the PCS is used as the maximum power of the ESS. By contrast, the allowable energy of the ESS based on the SOC is used:

$$\boldsymbol{S}_{limit} = \min(SOC_{limit}, PCS_{limit}, V_{lmit}, I_{limit}) \tag{13}$$

$$\begin{aligned} P_{ESS} &= \pm|\boldsymbol{S}_{limit}|cos\theta_{ESS}^{\circ} \\ Q_{ESS} &= \pm|\boldsymbol{S}_{limit}|sin\theta_{ESS}^{\circ} \end{aligned} \tag{14}$$

If the calculated complex power is less than the maximum power of the ESS ($|\boldsymbol{S}_{ESS}| < |\boldsymbol{S}_{limit}|$), the calculated value is used directly as the optimal consumed and supplied ESS energy. Otherwise, the maximum power of the ESS ($|\boldsymbol{S}_{limit}|$) is used.

An iterative approach is employed to determine the ESS energy for each phase based on the analytical solution derived in (11)–(14). Through this process, discrepancies between the analytical results and power-flow simulations, including numerical errors, are progressively corrected, and the procedure is repeated for all phases as described in (5). If the computed power violates voltage or current constraints, the algorithm reverts to the previous iteration; if such a violation occurs at the initial iteration, the ESS is not operated on the corresponding phase.

III. Economic Evaluation for Optimal Sizing

A. Battery wear out

This section introduces the economic indicators used to determine the optimal sizing of the ESS. ESSs generally employ lithium-ion secondary batteries, which degrade over time, reducing their lifespan. To calculate the degradation costs associated with ESS depreciation, the partial cycle method was used for ESS life prediction based on [12]. As shown in (15), one ESS lifecycle is defined as one full charge and discharge cycle ($E_{f,c}$, $E_{f,d}$), where E_{ESS} represents the ESS rated capacity. However, this approach does not fully reflect real ESS operation; therefore, a partial cycle approach was adopted, which calculates cycles by summing the energies from charging and discharging (E_c, E_d).

$$1\,cycle = \begin{cases} 1\,cycle_{full} & ;\ 2E_{ESS} = E_{f,c} + E_{f,d} \\ 1\,cycle_{partial} & ;\ 2E_{ESS} = \sum E_c + \sum E_d \end{cases} \tag{15}$$

$$D_{cycle} = \frac{SOH_0 - SOH_{limit}}{cyclc_{limit}} \tag{16}$$

In addition, an ESS is generally considered to have reached the end of its life when the state of health (SOH) has decreased to 70%. Thus, degradation per cycle (D_{cycle}) is defined as shown in (16). SOH_0 represents the initial capacity. SOH_{limit} represents the percentage of remaining capacity relative to the initial capacity.

B. Economic saving cost of imbalance

Without ESS operation, phase redistribution labor costs and customer-interruption costs will be incurred to mitigate the imbalance [8]-[9]. Moreover, it is assumed that transformer maintenance costs and additional customer-interruption costs occur because of the imbalance [3], [8]-[9]. By mitigating three-phase imbalance, ESS operation reduces these imbalance-related costs and further decreases power losses.

The economic savings from imbalance mitigation are defined in (17), where $CS_{imbalance}$ and CS_{loss} are calculated based on the reduction rates of the imbalance index and energy losses, respectively, along with their corresponding unit cost savings per improvement rate ($C_{imbalance}$). Here, $\Delta imbalance$ denotes the deviation of the imbalance index before and after ESS operation, and $\Delta loss$ represents the change in losses. C_{loss} denotes the power loss unit cost. The battery wear-out cost (C_{wear}), which is determined by multiplying the initial installation cost (IC_0) by the reduced capacity cycles is defined in (18). Consequently, (19) expresses the net profit ($Profit_{net}$).

$$\begin{aligned} CS_{imbalance} &= C_{imbalance} * \Delta imbalance \\ CS_{loss} &= C_{loss} * \Delta loss \end{aligned} \tag{17}$$

$$C_{wear} = IC_0 * \left(\frac{cycle_{partial,t}}{cycle_{limit}}\right) \tag{18}$$

$$Profit_{net} = CS_{imbalance} + CS_{loss} - C_{wear} \tag{19}$$

C. Economic analysis for optimal sizing

Generally, owing to the high initial installation and maintenance costs, an ESS cannot be deployed with unlimited capacity. The economic analysis indicators are computed as follows.

$$NPV = -IC_0 + \sum_{1}^{y} \frac{Profit_{net} - O\&M}{(1+r)^y} \tag{20}$$

$$LCOE = \frac{IC_0 + \sum_1^y O\&M}{\sum_1^y E_{ESS}} \tag{21}$$

where IC_0 is the initial cost of ESS and its PCS, $O\&M$ denotes the annual maintenance cost, r is the discount rate. y is the operating year.

The net-present value (NPV) in this study is calculated by subtracting the degradation costs from the annual profit, based on the initial cost and profit as (20). The payback period (PBP) can be derived using the NPV. The levelized cost of energy (LCOE) represents the total cost per unit of energy produced by the ESS. LCOE is calculated by dividing all costs incurred over the entire investment period by the total energy output generated as (21).

$$Optimal\ Capacity = \underset{E_{ESS}\in[E_{min},E_{maax}]}{\arg\max}\ NPV(E_{ESS}) \tag{22}$$

As the ESS capacity increases, the installation cost rises accordingly, whereas smaller capacities yield less improvement in imbalance mitigation. Consequently, the optimal ESS capacity is defined as the capacity that provides the maximum NPV, as expressed in (22), where E_{min}, E_{max} denotes the ESS min and max capacity range.

IV. CASE STUDY

A. Input data and assumption

This section introduces the input data and assumptions used in the simulation. An IEEE 34-bus test feeder is used as the test system, as shown on Fig. 2. To simulate real conditions, actual residential, industrial, and commercial loads and PV-generation profile data are employed in the test system [10]-[11]. The scheduling algorithm is updated every 15 min to align with the Energy Management System or Automatic Generation Control operations. The simulation is performed using MATLAB/ OpenDSS.

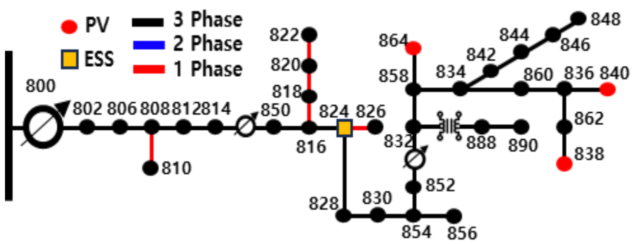

Figure 2. Modified IEEE-34 bus test feeder

TABLE I. INPUT PARAMETER

Content	Values	Content	Values
Over/under $\lvert \boldsymbol{I_{avg}} \rvert$ (%)	A: 36.0/64.0 B: 63.3/36.7 C: 27.1/72.9	I_{sc} (A)	A: 287.1 B: 292.8 C: 279.7
V_{max}(V)	1.05 PU	V_{min}(V)	0.95 PU
Unbalance Criteria (A)	52	Initial Cost of ESS (IC_0) ($/kWh)	160
Initial SOC (%)	50	O&M cost (year $/kWh)	5.07
ESS Capacity (kWh)	50-400	Discount rate (%)	5
PCS power	0.5 C-rate	C_{loss} ($/kWh)	0.1
Round trip efficiency (%)	95	$C_{imbalance}$ (%/kWh)	1946
PV power (kW)	100	D_{cycle} (%)	0.0107
PV penetration level	20%	Total Life cycle	2800

Table I lists the input parameters. The ESSs are placed at bus 824. The optimal ESS capacity is determined by exploring a range from 50 kWh to 400 kWh. It is combined with the 0.5 c-rate PCS, which has a 2-h maximum discharge. Single-phase PV systems are located on buses 864.A, 838.B and 840.C with 20% penetration level. The unit installation cost of the ESS is 160 $/kWh, and the O&M unit cost is 5.07 year $/kWh [8]-[13]. The discount rate for the NPV is 5%, and $C_{imbalance}$ is 1,946 [8-9]. C_{loss} is set to a typical value of 0.1 $/kWh. Using partial cycle method, D_{cycle} is set as 0.0107% [12]. The short-circuit current (I_{SC}) is set according to the IEEE test feeder analysis [13]. The voltage magnitude of all buses remains within ±5% of the 1.0 P.U.

B. Annual operation for optimal ESS sizing

This subsection presents the imbalance indicators and economic outcomes for various ESS capacity levels to identify the optimal ESS capacity. Figs. 3(a)–(b) show the annual average object and CUF. The sensitivity represents the average index value per unit of ESS energy used. As the ESS capacity increases, more energy is utilized, resulting in a corresponding decrease in both indicators. However, due to cost constraints, installing a high-capacity ESS is not always economically feasible. Therefore, considering the above trends, the subsequent analysis examines how this interaction between energy utilization and cost affects economic performance.

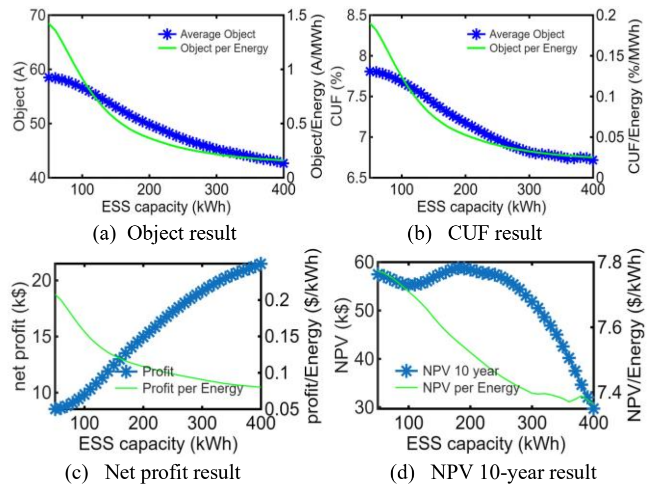

(a) Object result (b) CUF result

(c) Net profit result (d) NPV 10-year result

Figure 3. Optimal ESS capacity determination results

Fig. 3(c) presents the annual net profit. As the ESS capacity increases, the net profit rises. Although larger capacities yield higher profits, the incremental profit is outweighed by the corresponding wear-out cost. Furthermore, as the ESS capacity decreases, sensitivity increases, making the system more susceptible to variations in input parameters. Consequently, scenario variations can cause large deviations in the outcomes, implying that smaller ESS sizes are more vulnerable to economic uncertainty. Fig. 3(d) shows the 10-year NPV results. Considering both profit and degradation costs, the NPV reaches its maximum at an ESS capacity of 180 kWh. Therefore, as the 180 kWh capacity exhibits moderate sensitivity across all indicators and yields the highest NPV, it is selected as the optimal capacity for the current scenario.

C. Optimal ESS Operation results

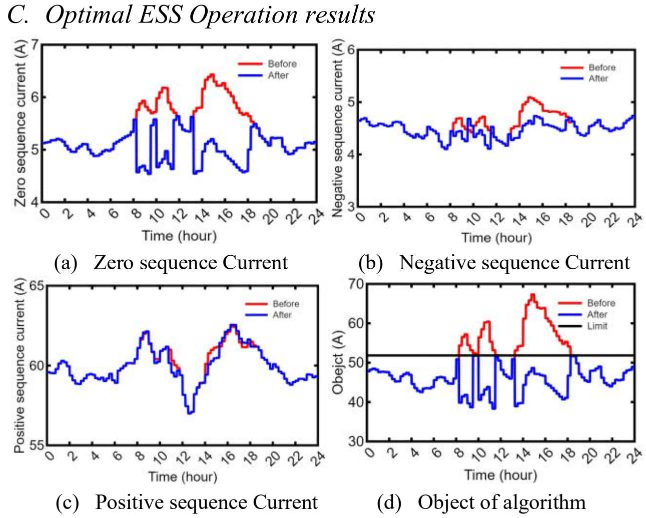

(a) Zero sequence Current (b) Negative sequence Current

(c) Positive sequence Current (d) Object of algorithm

Figure 4. Daily ESS Scheduling operation results

This subsection presents the algorithmic results obtained using the determined optimal ESS capacity. For validation, a typical day (Day 221) from the one-year simulation period is selected to show the details of the ESS operation. Fig. 4 shows the symmetrical component currents and the object of the algorithm on Day 221. The $\left|\boldsymbol{I}^{(0)}\right|$ and $\left|\boldsymbol{I}^{(-)}\right|$ values indicate the imbalance, which increases from the morning to 3 PM. However, $\left|\boldsymbol{I}^{(+)}\right|$ shows a trend like that of $\left|\boldsymbol{I}_{a,b,c}\right|$ before and after the ESS operation. This indicates that the algorithm can adjust and improve the imbalance without disrupting the load-current magnitude. Consequently, the object ($\left|\boldsymbol{I}^{(0)}\right|^2 + \left|\boldsymbol{I}^{(-)}\right|^2$) follows a similar decreasing trend as the value of $\left|\boldsymbol{I}^{(0)}\right|$ and $\left|\boldsymbol{I}^{(-)}\right|$. During off-peak times, when the object is below the unbalance criteria, the ESS is not operated. Overall, the object is well maintained below the unbalanced criteria.

TABLE II. 10-YEAR OPERATION RESULTS

Imbalance Indices	Value	Economic Indices	Value
Object Before (A)	63.37	Initial Cost (k$)	86.4
Object After (A)	52.27	PBP (year)	6
CUF Before (%)	8.12	Wear-out Cost (k$)	15.27
CUF After (%)	7.22	NPV (k$)	59.67
Loss Before (kW)	383.24	LCOE ($/kWh)	0.135
Loss After (kW)	353.17	Profit/Energy ($/kWh)	0.275
Used ESS energy (kWh)	69.77	BCR-wear cost (%)	9.65
Battery degradation (%)	4.7	BCR-total cost (%)	1.81

Table III presents the 10-year operational results obtained using the optimal ESS capacity. The imbalance indicators summarize the average values over the 10-year period. The object exhibits the greatest improvement, and as a secondary effect, power losses are reduced by approximately 8%. In terms of economic indicators, the PBP is six years, and the NPV reaches approximately 59,000 $ indicating that ESS-based three-phase imbalance mitigation is economically feasible. However, when installation costs are additionally considered, the benefit–cost ratio (BCR) is approximately 5.3 times smaller than that based on depreciation only, revealing the significant impact of capital cost on the overall profitability of ESS operation.

Thus, if an ESS is already installed and operational, the system can effectively achieve imbalance-mitigation benefits without requiring substantial additional investment. Furthermore, the battery capacity degradation is limited to 4.7%, suggesting that substantially more ESS energy can be utilized within its lifetime. Since this study focuses solely on imbalance mitigation, further participation in ancillary service markets or energy arbitrage programs could enhance the overall economic return. Consequently, distribution system operators should consider an appropriate trade-off between ESS capacity and the level of imbalance mitigation, given the associated economic effects.

V. CONCLUSION

This study proposes a methodology for ESS operation and optimal capacity determination aimed at mitigating three-phase imbalance. Given the high installation cost of ESSs, identifying the optimal capacity through economic evaluation is essential. The required ESS energy for three-phase balancing was derived by minimizing a symmetrical component–based objective function. The proposed algorithm was validated using a modified IEEE 34-bus test feeder. To determine the optimal capacity, an economic analysis considering both battery degradation and imbalance-mitigation savings was conducted. The proposed ESS operation algorithm, based on the optimal capacity, was validated, and its economic feasibility was demonstrated through a 10-year simulation. This study is expected to promote further research on ESS-based imbalance mitigation in distribution systems.

Future work can be extended in several directions. First, the proposed algorithm can be integrated with an ESS location optimization problem by identifying the spatially distributed imbalance within the network. Based on the ESS location optimization results, scenario-based analyses can be conducted to assess the generalizability of the proposed algorithm. Through coordination with higher-level management systems, the currently fixed threshold values can be operated using an adaptive thresholding scheme. Furthermore, beyond standalone ESS operation, the algorithm can be extended to scenarios coordinated with devices such as inverter-based resources and soft open points.

ACKNOWLEDGMENT

This research was supported by Korea Electric Power Corporation.(Grant number : R25XO02-5)

REFERENCES

[1] T. Adefarati and R.C. Bansal, "Integration of renewable distributed generators into the distribution system: A review," IET Renewable Power Generation, vol. 10, no. 7, pp. 873-884 2016.

[2] M.W. Siti, D.V. Nicolae, A.A. Jimoh and A. Ukil, "Reconfiguration and load balancing in the LV and MV distribution networks for optimal performance," IEEE Trans.Power Del., vol. 22, no. 4, pp. 2534-2540 2007.

[3] Sharma, A., Bharat Singh Rajpurohit, and S. N. Singh. "A review on economics of power quality: Impact, assessment and mitigation." Renewable and sustainable energy reviews 88 (2018): 363-372.

[4] F. Geth, J. Tant, R. Belmans, and J. Driesen, "Balanced and unbalanced inverter strategies in battery storage systems for low-voltage grid support," IET Generation, Transmission & Distribution, vol. 9, no. 10, pp. 929–936, Jul. 2015

[5] Hashmi, Md Umar, et al. "Towards phase balancing using energy storage." arXiv preprint arXiv:2002.04177 (2020).

[6] Akdogan, Mehmet Emin, and Sara Ahmed. "Novel compensation methods using energy storage system (ESS) in islanded unbalanced single-/three-phase multimicrogrids." IEEE Transactions on Industry Applications 58.4 (2022): 5457-5468.

[7] Liu, Yu, et al. "The prospects of energy storage technology development in China: Long-term analysis of economic and environmental benefits." Journal of Energy Storage 138 (2025): 118568.

[8] Soltani, Shirin, Saeed Soltani, and Masoud Rashidinejad. "Distribution systems reliability improvement using optimal phase balancing and economic analysis." Electrical Engineering 107.4 (2025): 4471-4482.

[9] Lin, Chia-Hung, et al. "Optimal phase balancing in electricity distribution feeders using mixed-integer linear programming." Sustainability 15.5 (2023): 4473.

[10] Zenodo, Open data web site. Accessed: Oct 2025. [Online]. Available: https://zenodo.org/record/3899018#.Ybwp9b1ByUk

[11] Korea Public Data Portal: Ministry of the Interior and Safety, South Korea web site. Accessed: Oct 2025. [Online]. Available: https://www.data.go.kr/data/15025486/fileData.do

[12] Baek, Min-Kyu, et al. "Optimal sizing of battery/supercapacitor hybrid energy storage systems for frequency regulation." Journal of Electrical Engineering & Technology 17 (2022): 111-120

[13] Kersting, W. H., and Greg Shirek. "Short circuit analysis of IEEE test feeders." *PES t&d 2012*. IEEE, 2012.